



SYNTHESIS AND CHARACTERIZATION OF MALTOL MODIFIED MAGNETITE NANOPARTICLES

Daniela C. CULIȚĂ,^{a*} Gabriela MARINESCU,^a Luminița PATRON^a and Lucian DIAMANDESCU^b

^aInstitute of Physical Chemistry "Ilie Murgulescu", Splaiul Independentei 202, 060021 Bucharest, Roumania

^bNational Institute of Materials Physics, 105 bis Atomistilor Street, P.O. Box. Mg-7, Bucharest-Magurele, R-077125, Roumania

Received July 27, 2009

Maltol functionalized magnetite nanoparticles were synthesized by in situ decomposition of the precursor – polynuclear coordination compounds containing maltol as a ligand. X-ray diffraction, Mössbauer spectroscopy, Fourier transform infrared spectroscopy were used to characterize the nanoparticles system. The magnetic properties were measured by means of a superconducting quantum interference device. The particle size of the magnetite nanoparticles was estimated to be about 8 nm. At room temperature the magnetite nanoparticles were proved to be superparamagnetic with saturated magnetization of 67.29 emu/g and blocking temperature of about 175 K.

INTRODUCTION

Synthesis and processing of nanoparticles with controlled chemical and structural properties are the main features for the design of nanoobjects. Magnetic nanoparticles with specific properties have been extensively studied due to their potential applications in several areas, including in-vivo drug delivery,^{1,2} hyperthermia,^{3,4} MRI contrast agent,^{2,5,6} immunoassay,⁶ immunomagnetic array,⁷ magnetic storage,⁸ magnetic ink printing,⁹ microwave absorption¹⁰ and in-vitro cell separation.¹¹ Although studies on the magnetite particle formation have been markedly advanced, the preparation of well-dispersed magnetite nanoparticles with narrow size distribution still remain an open area. Among various synthesis methods developed till now, wet chemical methods have been widely used to produce magnetite nanoparticles. The most used is the coprecipitation method which consists in ageing stoichiometric mixtures of ferrous and ferric salts in aqueous media, yielding homogeneous spherical particles of magnetite or maghemite. It has been shown that by adjusting the pH and the

ionic strength of the precipitation medium, it is possible to control the particle mean size.¹² Modification of this method, implying the presence of other substances, turn into biocompatible magnetic nanoparticles. In some of our previous papers we showed that using this modified method it is possible to functionalize the surface of the magnetic nanoparticles with various types of biomolecules – bile acids,¹³ aminoacids.^{14,15}

In order to extend these studies, in this work we tried to obtain very fine functionalized magnetite nanoparticles by the coprecipitation method in the presence of 2-methyl-3-hydroxy-4H-pyran-4-one, well known as maltol. To the best of our knowledge, the use of maltol for this purpose have not been reported in the literature up to now. It is well known that maltol has a potentially strong biological activity while forming complexes with metal ions, some of them being tested as new drugs.¹⁶ The most promising ones are maltol complexes with vanadium (insulin mimetic properties)^{17,18} and iron(III) (iron deficiency anaemia) ions.¹⁹ On the other hand, maltol has been suggested as an oral agent that can be used to remove the excess of iron ions in thalassaemia or

* Corresponding author: danaculita@yahoo.co.uk

haemochromatosis.²⁰ It has been also shown that it can also reduce the aluminium level in the body, possibly slowing down the progress of different dementias.²⁰

EXPERIMENTAL

Synthesis of magnetite nanoparticles

Iron sulphate ($\text{FeSO}_4 \cdot 7\text{H}_2\text{O}$), iron nitrate ($\text{Fe}(\text{NO}_3)_3 \cdot 9\text{H}_2\text{O}$) of reagent grade, maltol and sodium hydroxide (aqueous solution), were obtained from Merck. All chemicals were used as received.

To an aqueous solution of Fe(III) and Fe(II) salts, a solution of maltol was added to obtain the molar ratio 2Fe(III) : 1Fe(II) : 8Maltol. The dark red solution was kept at room temperature for 15 minutes under vigorous stirring. Thereafter an aqueous NaOH solution was added dropwise into the dark-red solution to bring the pH to ~ 12 . After stirring for ~ 1 hour at 80°C , the final product – black suspension – was thoroughly washed with deionized water to neutral pH and finally dried. The black powder formed exhibits a positive magnetic behaviour in the presence of a permanent magnet.

Characterization of the products

Phase identification was performed at room temperature using an X-ray diffractometer (DRON-2) using CuK_α radiation and a graphite monochromator in the diffracted beam. A step scanning technique was applied with a step width of 0.04° in the 2θ range of 20 – 70° . The crystalline phase identification was performed using ICSD files system. Magnetic characterization was performed with a commercial superconducting quantum interference device (SQUID) magnetometer. Mössbauer spectra were recorded at room temperature on a standard Mössbauer spectrometer linked to a data acquisition and processing facility. The source was ^{57}Co in Rhodium matrix with initial activity of 50 mCi. The absorber thickness was 7 mg Fe cm^{-2} . TEM images to determine the size and morphology of the synthesized magnetic powders were collected with an electronic microscope JEOL 200 CX operated at 200 kV. The TEM specimens have been prepared by crushing and deposition of the resulting powder onto holey membrane Cu grids. FTIR spectra in the range 400 – 4000 cm^{-1} (Bio-Rad FTS-135 spectrophotometer) were carried out in order to evidence the nature of the chemical bonds formed.

RESULTS AND DISCUSSION

The magnetization of ferrimagnetic materials, such as magnetite, is very sensitive to the microstructure of a particular sample. If a sample consists of small particles, its total magnetization decreases with particle size because of increasing dispersion on the exchange integral, and finally reaches the superparamagnetic state when each particle acts as a single-domain dipole moment,

with suppressed exchange interaction between particles. Figure 1 presents room temperature magnetization as a function of applied magnetic field for the as-prepared nanomagnetite. The superparamagnetic behaviour is documented by the magnetization measured at 300 K. There is almost immeasurable coercivity for Fe_3O_4 at room temperature, this indicates that the Fe_3O_4 particles are superparamagnetic and nanosized. The saturation magnetization (M_s) at 300 K is about 67.29 emu/g , lower than that of bulk magnetite particles ($M_{\text{bulk}} = 92 \text{ emu/g}$).²¹ The hysteresis of magnetization at 5 K is shown in Figure 2 with small coercivity and remanence of magnetization. The inset of the Figure 2 shows the hysteresis of magnetization versus magnetic field up to 50000 Oe, indicating a saturating tendency of magnetization around 50000 Oe. However, the value of magnetization (M_s) at 5 K and 50000 Oe is 77.14 emu/g . The possible causes of the decrease in M_s compared with bulk magnetite could be chemical changes on the surface, magnetic degradation of the surface or the decrease of particle size.

Furthermore, in the FTIR spectra of the sample (Figure 3), besides the characteristic band from Fe_3O_4 at about 577 cm^{-1} , there were four absorption bands also observed at about 1572, 1471, 1277 and 1206 cm^{-1} , the former two bands correspond to the C=O and C=C bond vibrations, respectively, and the last two bands to the C-O deformation vibrations of the organic skeleton.^{17,22} These results suggest that the maltol molecules irreversibly adsorbed on the surface of Fe_3O_4 particles even after careful washing. So, the magnetically inactive layer of the magnetic particle and the decreasing of the particle size seem to be responsible for the lower saturation magnetization of the sample.

The temperature dependence of the magnetization was measured using zero-field cooling (ZFC) and field cooling (FC) procedures, in an applied magnetic field of 100 Oe, between 5 and 300 K (Figure 4). Above 170 K, the magnetization decreases with increasing temperature in both the ZFC and the FC case. At lower temperatures, the magnetization increases monotonically with decreasing temperature for the FC case, whereas the ZFC magnetization passes through a maximum at 175 K, which can be associated with the blocking temperature.

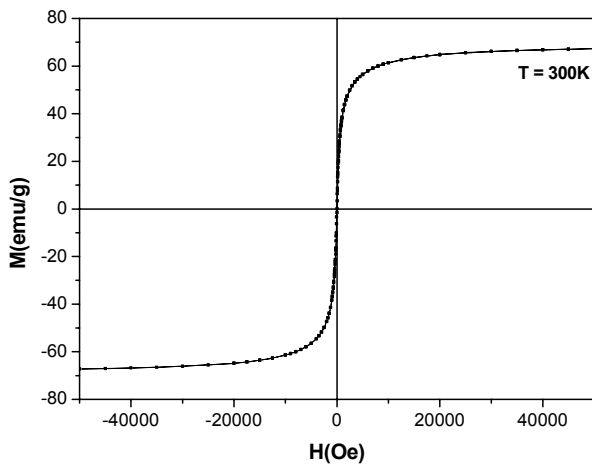


Fig. 1 – Magnetization curves for the maltol functionalized magnetite at 300 K.

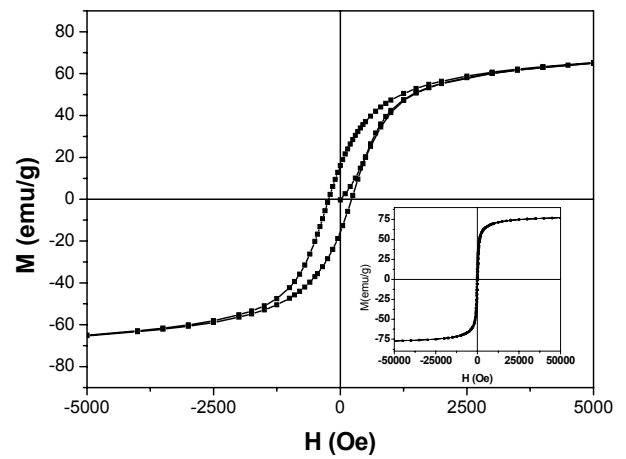


Fig. 2 – Hysteresis of magnetization at 5 K in the low field range. The inset exhibits the example of the same up to 50000 Oe.

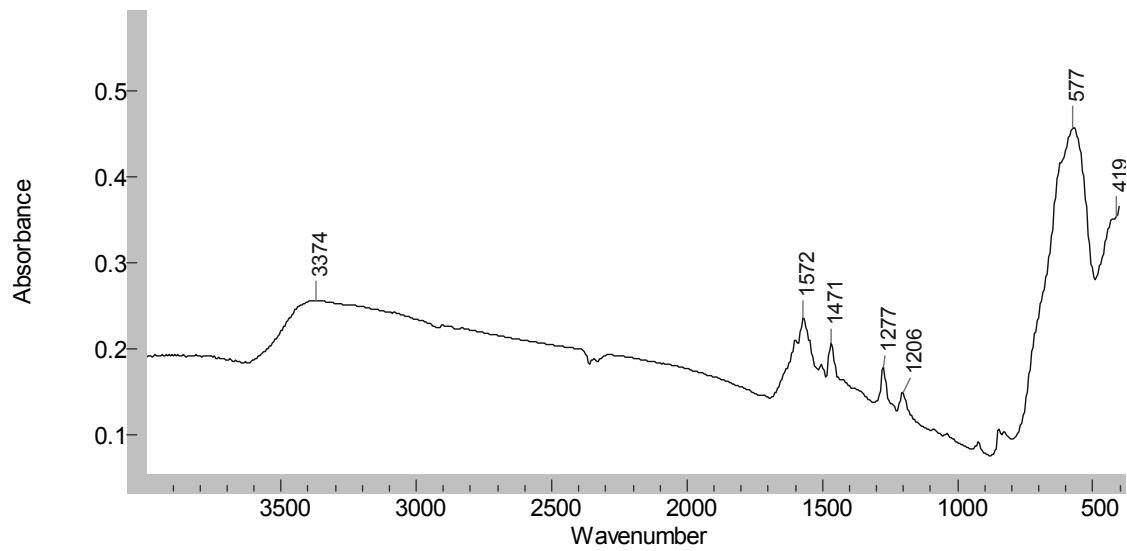


Fig. 3 – FTIR spectra of the maltol functionalized magnetite.

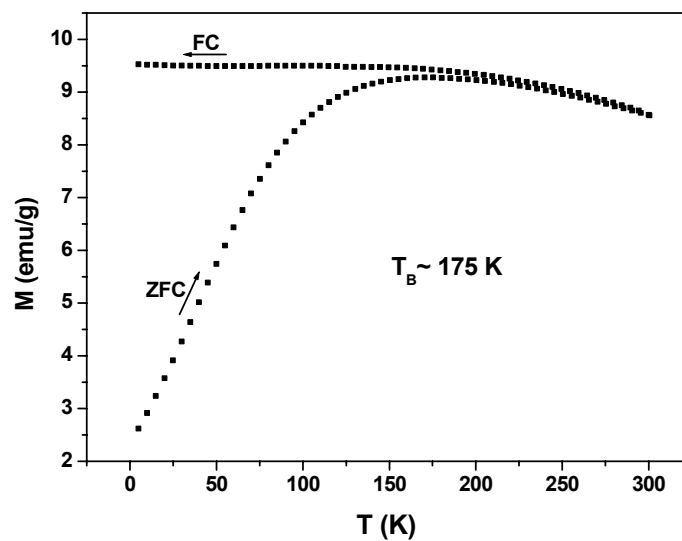


Fig. 4 – Magnetization vs. temperature for maltol functionalized magnetite.

The crystalline structure and phase purity were determined by powder XRD. The diffraction peaks of the functionalized magnetite sample are characteristic for a spinel structure of nanoscaled magnetite (Figure 5). The crystallite sizes calculated applying the Debye-Scherrer formula based on the half-width of the most intense peak (311) of the magnetite phase were about 8 nm, in agreement with those estimated by TEM images (Figure 6).

The Mössbauer spectrum of the maltol coated magnetite recorded at 300K (Figure 7) exhibits an unusual shape. A typical Mössbauer spectrum of polycrystalline magnetite consists in two magnetic sextets²³ corresponding to iron ions in tetrahedral and octahedral sites of the cubic magnetite structure. When the magnetite particle dimension drops reaching the nanometric scale, Mössbauer spectrum collapses as the result of superparamagnetic effects.^{24,25} The process is controlled by a spin relaxation time $\tau = \tau_0 \exp(KV/kT)$, for uniaxial magnetic anisotropy, where K is the magnetic

anisotropy density, V is the volume of the particle, T is the temperature, k is Boltzmann's constant, and τ_0 is a constant characteristic of the material. This relaxation time causes the spectra to change gradually from magnetically split spectrum for micrometric or bulk magnetite particles to a collapsed superparamagnetic spectrum observed in the case of very small particles. Our Mössbauer spectrum coming from magnetite nanoparticles was best fitted with two significantly different components: a central doublet and a magnetic hyperfine field distributions. The quadrupole doublet corresponds to superparamagnetic magnetite particles and represents $\sim 56\%$ of the total area. The quadrupole splitting of 0.67 mm s^{-1} together with the corresponding isomer shift of 0.31 mm s^{-1} represent the contribution of Fe^{3+} to the Mössbauer spectrum.²³ The magnetic hyperfine field distribution is given by the iron cations located in bigger particles ($>5 \text{ nm}$).

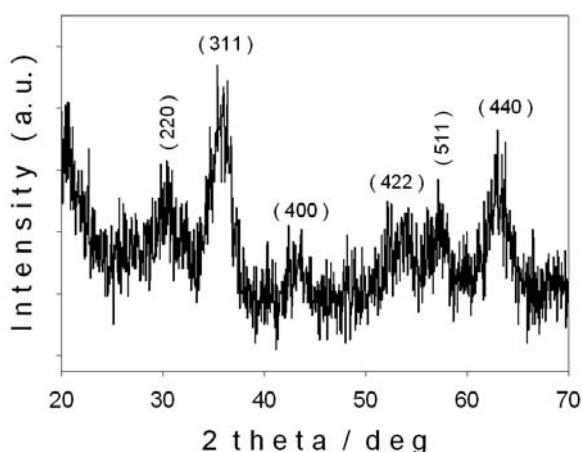


Fig. 5 – XRD patterns of maltol functionalized magnetite.

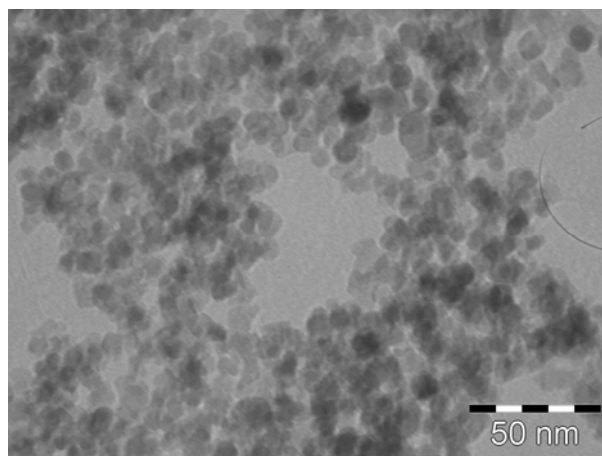
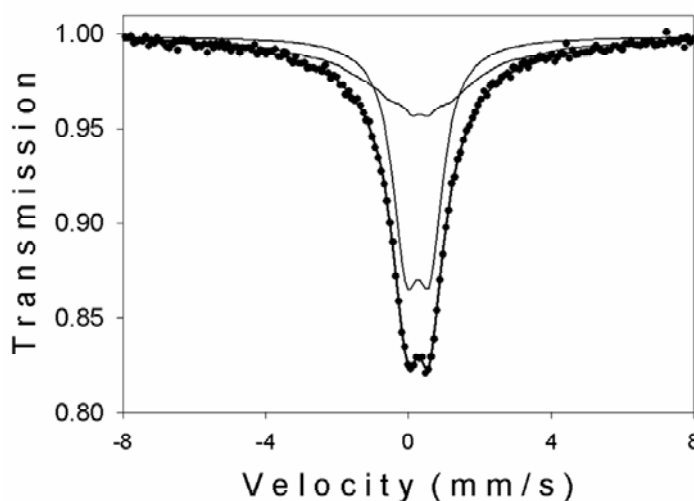


Fig. 6 – TEM image of the maltol functionalized magnetite.

Fig. 7 – Room temperature Mössbauer spectrum for the maltol functionalized magnetite.



CONCLUSION

Superparamagnetic magnetite nanoparticles functionalized by maltol were successfully synthesized in only one step by in situ decomposition of the coordination compound containing maltol as ligand. The FTIR spectra clearly confirmed the presence of maltol on the surface of magnetite nanoparticles and also the chemical nature of the bonds between the organic molecule (maltol) and iron cations in magnetite. The sample shows superparamagnetic behaviour at 300 K with a saturation magnetization, M_s , of 67.29 emu/g. The reduction of M_s from its bulk value, attributed partly to the presence of a magnetically inactive surface layer, is an additional proof for the chemisorption of the maltol on the surface of the magnetite. The average diameter of magnetite nanoparticles estimated from XRD and TEM was \sim 8nm. Furthermore, magnetite nanoparticles synthesized in this work could be useful for biomedical applications due to their small particle size and superparamagnetic property at room temperature.

Acknowledgments: This work was financially supported by the CNCSIS - Ideas Project no. 158 / 2007. The authors thank Dr. Marcel Feder and Dr. Corneliu Ghica from National Institute of Materials Physics for their assistance in the X-ray diffraction and TEM measurements.

REFERENCES

1. P. Tartaj, M. P. Morales, S. Veintemillas-Verdaguer, T. Gonzalez-Carreno and C. J. Serna, *J. Phys. D: Appl. Phys.*, **2003**, *36*, R182 – R197.
2. T. Neuberger, B. Schöpf, H. Hofmann, M. Hofmann and B. Von Rechenberg, *J. Magn. Magn. Mater.* **2005**, *293*, 483 - 496.
3. U. Hafeli, G. Pauer, S. Failing and G. Tapolsky, *J. Magn. Magn. Mater.*, **2001**, *225*, 73-78.
4. M. Gonzales and K. M. Krishnan, *J. Magn. Magn. Mater.*, **2005**, *293*, 265 - 270.
5. B. Chertok, B. A. Moffat, A. E. David, F. Yu, C. Bergenamm, B. D. Ross and V. C. Yang, *Biomaterials*, **2008**, *29*, 487 – 496.
6. J. R. McCarthy and R. Weissleder, *Adv. Drug Delivery Rev.*, **2008**, *60*, 1241-1251.
7. C. V. Mura, M. I. Becker, A. Orellana and D. Wolff, *J. Immuno. Methods*, **2002**, *260*, 263-271.
8. A. Chakraborty, *J. Magn. Magn. Mater.*, **1999**, *204*, 57 - 60.
9. V. T. Peikov, K. S. Jeon and A. M. Lane, *J. Magn. Magn. Mater.*, **1999**, *193*, 307 - 310.
10. M. S. Pinho, M. L. Gregori, R. C. R. Nunes and B. G. Soares, *Polym. Degrad. Stab.*, **2001**, *73*, 1 - 5.
11. S. Sieben, C. Bergemann, A. Lübe, B. Brockmann and D. Rescheleit, *J. Magn. Magn. Mater.*, **2001**, *225*, 175 - 179.
12. J. P. Jolivet, "Metal Oxide Chemistry and Synthesis: From Solutions to Solid State", Wiley, New York, US, 2000.
13. D. C. Culiță, L. Patron, V. S. Teodorescu and I. Balint, *J. Alloys Compd.*, **2007**, *432*, 211–216.
14. G. Marinescu, L. Patron, D. C. Culiță, C. Neagoe, C. I. Lepadatu, I. Balint, L. Bessais and C. B. Cizmaș, *J. Nanoparticle Res.*, **2006**, *8*, 1045–1051.
15. D. C. Culiță, G. Marinescu, L. Patron, O. Carp, C. B. Cizmaș and L. Diamandescu, *Mater. Chem. Phys.*, **2008**, *111*, 381–385.
16. K. H. Thompson and C. Orvig, *Coord. Chem. Rev.*, **2001**, *219*, 1033 - 1053.
17. M. Melchior, S. J. Rettig, B. D. Liboiron, K. H. Thompson, V. G. Yuen, J. H. McNeill and C. Orvig, *Inorg. Chem.*, **2001**, *40*, 4686 - 4690.
18. J. H. McNeill, V. G. Yuen, H. R. Hoveyda and C. Orvig, *J. Med. Chem.*, **1992**, *35*, 1489 - 1491.
19. M. T. Ahmet, C. S. Frampton and J. Silver, *J. Chem Soc. Dalton Trans.* **1988**, 1159 - 1163.
20. S. I. Ahmed, J. Burgess, J. Fawcett, S. A. Parsons, D. R. Russell and S.H. Laurie, *Polyhedron*, **2000**, *19*, 129 - 135.
21. G. F. Zou, K. Xiong, C. L. Jiang, H. Li, T. W. Li, J. Du and Y. T. Qian, *J. Phys. Chem. B*, **2005**, *109*, 18356 - 18360.
22. M. C. Barret, M. F. Mahon, K. C. Molloy, J. W. Steed and P. Wright, *Inorg. Chem.*, **2001**, *40*, 4384-4388.
23. N. N. Greenwood and T. D. Gibb, "Mössbauer Spectroscopy", Chapman and Hall, London, 1971.
24. G. F. Goya, *Solid State Communications*, **2004**, *130*, 783 - 787.
25. H. Pardoe, W. Chua-Anusorn, T. G. St. Pierre and J. Dobson, *J. Magn. Magn. Mater.*, **2001**, *225*, 41 - 46.

